FLOWERING BHLH transcriptional activators control expression of the photoperiodic flowering regulator *CONSTANS* in *Arabidopsis*

Shogo Ito[a], Young Hun Song[a], Anna R. Josephson-Day[a], Ryan J. Miller[a], Ghislain Breton[b,1], Richard G. Olmstead[a], and Takato Imaizumi[a,2]

[a]Department of Biology, University of Washington, Seattle, WA 98195-1800; and [b]Section of Cell and Developmental Biology, Division of Biological Sciences, University of California at San Diego, La Jolla, CA 92093

Edited by Peter H. Quail, University of California, Berkeley, Albany, CA, and approved January 17, 2012 (received for review November 16, 2011)

Many plants monitor day-length changes throughout the year and use the information to precisely regulate the timing of seasonal flowering for maximum reproductive success. In *Arabidopsis thaliana*, transcriptional regulation of the *CONSTANS* (*CO*) gene and post-translational regulation of CO protein are crucial mechanisms for proper day-length measurement in photoperiodic flowering. Currently, the CYCLING DOF FACTOR proteins are the only transcription factors known to directly regulate *CO* gene expression, and the mechanisms that directly activate *CO* transcription have remained unknown. Here we report the identification of four *CO* transcriptional activators, named FLOWERING BHLH 1 (FBH1), FBH2, FBH3, and FBH4. All FBH proteins are related basic helix–loop–helix-type transcription factors that preferentially bind to the E-box *cis*-elements in the *CO* promoter. Overexpression of all *FBH* genes drastically elevated *CO* levels and caused early flowering regardless of photoperiod, whereas *CO* levels were reduced in the *fbh* quadruple mutants. In addition, FBH1 is expressed in the vascular tissue and bound near the transcription start site of the *CO* promoter in vivo. Furthermore, *FBH* homologs in poplar and rice induced *CO* expression in *Arabidopsis*. These results indicate that FBH proteins positively regulate *CO* transcription for photoperiodic flowering and that this mechanism may be conserved in diverse plant species. Our results suggest that the diurnal *CO* expression pattern is generated by a concert of redundant functions of positive and negative transcriptional regulators.

photoperiodism | developmental transition | circadian clock

The precise alignment of flowering timing with season is crucial for successful reproduction. Various plants monitor photoperiod (day-length) changes throughout the year and use the information to regulate the timing of flowering (1). Photoperiodic flowering regulation is mediated by complex interactions between internal timekeeping mechanisms termed "circadian clocks" and "external environmental stimuli," such as light and temperature (2). In *Arabidopsis thaliana*, the circadian-clock–regulated transcriptional regulation of the *CONSTANS* (*CO*) gene and the light-dependent posttranslational regulation of CO protein are the most crucial mechanisms for day-length measurement in photoperiodic flowering (3–6). In this mechanism, expression of the floral integrator gene *FLOWERING LOCUS T* (*FT*) is induced only when the CO protein expression coincides with the presence of light. FT protein synthesized in the leaf vasculature that moves to the shoot apical meristem (SAM) is thought to be the long-sought mobile floral induction signal "florigen" (7). At the SAM, FT binds to the bZIP transcription factor FD to initiate the expression of the floral meristem identity genes (8, 9). In addition, the *CO*/*FT* functional modules, as well as the daily expression patterns of *CO* homologs in flowering regulation, are widely conserved in many plant species (10, 11). Thus, to understand general seasonal flowering mechanisms, it is important to understand the regulatory mechanisms of the *CO*/*FT* module.

To induce *FT* under specific day-length conditions, the timing of daily *CO* transcription needs to be precisely regulated. *Arabidopsis* possesses a number of factors that regulate *CO* transcription, such as GIGANTEA (GI), FLAVIN-BINDING, KELCH REPEAT, F-BOX 1 (FKF1), RED AND FAR-RED INSENSITIVE 2 (RFI2), LONG VEGETATIVE PHASE 1 (LOV1), FIONA1 (FIO1), LIGHT-REGULATED WD1 (LWD1)/2, and CYCLING DOF FACTOR (CDF) proteins (12–21). The timing of the expression of all these genes is precisely regulated throughout the day by the circadian clock. Except for GI and FKF1, all of them are negative regulators of *CO*, and the mechanisms by which these proteins regulate *CO* transcription are largely unknown (12–21). Among these transcriptional regulators of *CO*, CDF1 is the only transcription factor known to directly bind to the *CO* promoter (15, 22), although LOV1 and FIO1 also contain DNA-binding motifs (18, 19). Overexpression of all *CDF* genes led to a decrease of *CO* transcripts and delayed flowering in long days (15, 21, 22). CDF1 was originally identified as an interacting protein of the FKF1 Kelch-repeat domain where a potential substrate for protein degradation binds (15). FKF1 absorbs blue light through its Light, Oxygen, or Voltage (LOV) domain (14, 22), and after light absorption, FKF1 binds to GI and functions as an SCF E3 ubiquitin ligase complex to target CDF proteins for degradation on the *CO* promoter (15, 21, 22). This mechanism enables plants to induce *CO* during late afternoon under long-day (LD) conditions. All CDF proteins are *CO* transcriptional repressors, and no transcriptional activators have been yet identified. To elucidate the mechanisms by which daily *CO* expression is controlled in combination with the CDF repressors, we attempted to identify additional *CO* regulators. Here we report a set of transcriptional activators of *CO*.

Results

FBH1 and FBH2 Bind to the *CO* Promoter. Because the expression of all known *CO* regulators is controlled by the circadian clock (6), we screened the clock-regulated transcription factor library using a yeast one-hybrid assay (23). Using a *CO* promoter fragment (500 bp), we found one transcription factor that strongly increased *LacZ* reporter activity (Fig. 1*A*). The transcription factor (At1g35460) belongs to the basic helix–loop–helix (bHLH) transcription factor family and has not been previously characterized. There is a close homolog (At4g09180) to the bHLH (74.4% identity over the entire amino acid sequences) in the *Arabidopsis* genome; therefore, we included the homolog in our assay. As these two genes encode bHLH proteins that affect flowering time (as shown later), we named them *FLOWERING BHLH 1* (*FBH1*) and *FBH2*. Like FBH1, FBH2 increased LacZ activity, indicating that both proteins bind to the *CO* promoter in yeast (Fig. 1*A*). On the basis of the amino acid sequences of their bHLH domains, both proteins were predicted to

Author contributions: S.I. and T.I. designed research; S.I., Y.H.S., A.R.J.-D., and T.I. performed research; R.J.M., G.B., and R.G.O. contributed new reagents/analytic tools; S.I., Y.H.S., and T.I. analyzed data; and S.I. and T.I. wrote the paper.

The authors declare no conflict of interest.

This article is a PNAS Direct Submission.

[1]Present address: Department of Integrative Biology and Pharmacology, University of Texas Medical School, Houston, TX 77030.

[2]To whom correspondence should be addressed. E-mail: takato@u.washington.edu.

This article contains supporting information online at www.pnas.org/lookup/suppl/doi:10.1073/pnas.1118876109/-/DCSupplemental.

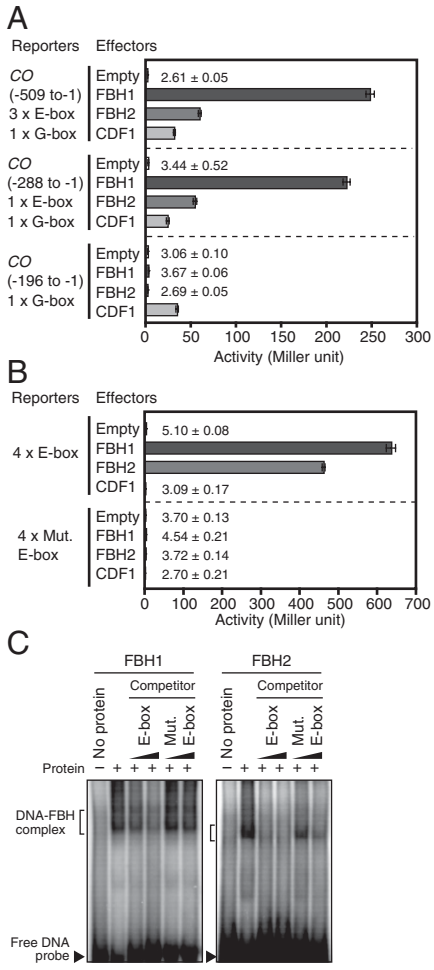

Fig. 1. FBH1 and FBH2 bind to the *CO* promoter. (*A*) Interaction of FBH1 and FBH2 with *CO* promoter in yeast. Bars represent β-galactosidase enzyme activities (Miller units) controlled by *CO* promoter fragments. The numbers on the left denote the region of the promoter included in each reporter construct (the *CO* transcription start site, +1). The number of E-box and G-box elements in each fragment is indicated. CDF1 binds to the Dof-binding site (−173 to −135) on the *CO* promoter (15). (*B*) Interaction of FBH1 and FBH2 with E-box. The 20 bp of the *CO* promoter fragment (−239 to −219) encompassing the E-box element (with or without a mutation) was repeated four times and then fused to the minimum promoter to drive *LacZ* expression. All data in *A* and *B* represent means ± SEM ($n = 15$). (*C*) EMSA of FBH1 and FBH2 proteins. The four E-box-repeat fragment used in *B* was radioactively labeled. The same fragment and the mutated E-box-repeat fragment were used as nonlabeled competitors in 1:20 and 1:100 ratios (labeled vs. nonlabeled DNA).

preferentially bind to an E-box *cis*-element rather than a G-box (24). The *CO* promoter fragment that we used contains three E-box elements and one G-box element. Analysis of truncated *CO* promoter fragments revealed that the shorter promoter fragment (−288 to −1), which contains one E-box and one G-box element, was sufficient for the FBH-dependent induction of the *LacZ* reporter (Fig. 1*A*). However, both FBH proteins failed to induce *LacZ* expression when the shortest *CO* promoter fragment (−196 to −1) containing one G-box element and Dof-binding sites was used (Fig. 1*A*) (15). CDF1 could induce *LacZ* expression in the same yeast strain (Fig. 1*A*), indicating that the shortest *CO* promoter fragment is functional. These results suggest that FBH1 and FBH2 bind to the region that contains E-box elements. To verify that the E-box is an FBH binding site, we used a synthetic promoter that possesses four repeats of the E-box elements derived from the *CO* promoter (named as "4× E-box") to control *LacZ* expression. Both FBH1 and FBH2 increased reporter activity (Fig. 1*B*). However, when the E-box elements were mutated ("4× Mut. E-box") (24), the FBHs no longer induced reporter expression. In addition, we further confirmed the direct binding of both FBH proteins to the same E-box elements by electrophoretic mobility shift assay (EMSA) (Fig. 1*C*). These results suggest that FBH1 and FBH2 bind to the E-box elements in the *CO* promoter in vivo.

FBH1 and FBH2 Are Activators in the *CO/FT* Photoperiodic Flowering Pathway. We postulated that if FBH1 and FBH2 are involved in *CO* transcriptional regulation in vivo, overexpression of FBHs could change *CO* expression levels, which consequently would alter flowering time. Therefore, we analyzed the flowering phenotype of *FBH1* and *FBH2* overexpressors (*35S:FBH1* and *35S:FBH2*, Fig. S1 *A–D*) under LD and short-day (SD) conditions. *FBH1* and *FBH2* overexpressors showed a distinct early flowering phenotype regardless of photoperiod (Fig. 2 *A–C*), which resembles that of the *CO* overexpressors (25). This result suggests that the *FBH* overexpressors may have increased levels of *CO*. As predicted, the *CO* expression levels were elevated in the *35S:FBH* lines in LD and SD (Fig. 2 *D* and *E* and Fig. S1 *O–Q*), indicating that both FBH1 and FBH2 induce *CO* transcription. Interestingly, even though the peak *CO* levels in the *35S:FBH* lines were almost 20 times higher than those in wild-type plants, the daily *CO* expression patterns in *35S:FBH*s were very similar to the wild-type *CO* patterns in LD and SD (compare the *CO* patterns in Fig. 2 *D* and *E* with those in Fig. S1 *E* and *F*). Because the *FBH* transcripts are constitutively expressed at high levels throughout the day in *35S:FBH*s, this result suggests that the transcriptional activity of FBHs may change throughout the day.

To determine the potential contribution of other *CO* regulators to *CO* expression in the *FBH* overexpressors, we surveyed the daily expression patterns of known *CO* regulator genes, such as *GI*, *FKF1*, *CDF1*, and *CDF2* (13, 15, 21, 22). Except for a slight reduction in the peak expression of *GI*, *FKF1*, *CDF1*, and *CDF2* in the *35S:FBH* lines, the expression patterns of these genes resembled the *35S:FBH*s and wild-type plants in LD and SD (Fig. S1 *G–N*). Our results indicated that elevated levels of *FBH*s directly and specifically increased the amount of *CO* transcripts.

To elucidate potential causes of the early flowering phenotype of the *FBH* overexpressors, we investigated expression levels of the major flowering-time regulators, which function downstream of *CO*. The abundance of *FT* mRNA was also highly increased in the *FBH* overexpressors in LD and SD (Fig. 2 *F* and *G* and Fig. S1*R*). *FLOWERING LOCUS C* (*FLC*) expression was slightly reduced, and *SUPPRESSOR OF OVEREXPRESSION OF CONSTANS* (*SOC1*) expression was not altered in the *35S:FBH* lines (Fig. S1 *S* and *T*) (25, 26). These results suggest that elevated *FT* levels may induce early flowering in the *35S:FBH* lines. To genetically evaluate this possibility, we introduced the *ft* mutation into the *35S:FBH1* line. The *35S:FBH1 ft* line showed an obvious late-flowering phenotype, which is similar to that of *ft*, in LD and SD (Fig. S2 *A–C*). This result supports the notion that the early flowering phenotype of *35S:FBH1* is mainly due to the increase in *FT* levels, which is likely caused by the elevated levels of *CO*.

We demonstrated that the elevated levels of *FBH1* and *FBH2* are directly associated with increased *CO* expression. To further analyze the *FBH*-dosage–dependent induction of *CO*, we used the estradiol-mediated *FBH* inducible system (*pER8-FBH1* and *pER8-FBH2*) (27). β-Estradiol was applied to 10-d-old transgenic and wild-type seedlings, and *FBH1*, *FBH2*, and *CO* gene expression was analyzed for 2 d (Fig. 2*H*). *CO* expression increased only in plants in which *FBH1* or *FBH2* expression was induced (Fig. 2 *I–L*). This result further indicates that the amounts of *FBH1* and *FBH2* control the amplitude of daily *CO* oscillation.

Because *CO* is expressed mainly in vascular tissues (Fig. 2*M*) (28, 29), we analyzed whether the *FBH* overexpression affects the *CO* spatial expression pattern using the *CO* promoter-fused β-glucuronidase (*CO:GUS*) reporter (28). CO:GUS activity in the *35S:FBH* seedlings was higher than that in the wild-type *CO:GUS* plants but was still restricted mainly to the vascular tissues (Fig. 2 *M–O*), even though both *FBH1* and *FBH2* are ubiquitously expressed (Fig. S1 *A–D*). In addition, ectopic GUS activity was observed in stomata in leaves and root tips (Fig. 2 *M–O* and Fig. S2 *D* and *E*). These

PLANT BIOLOGY

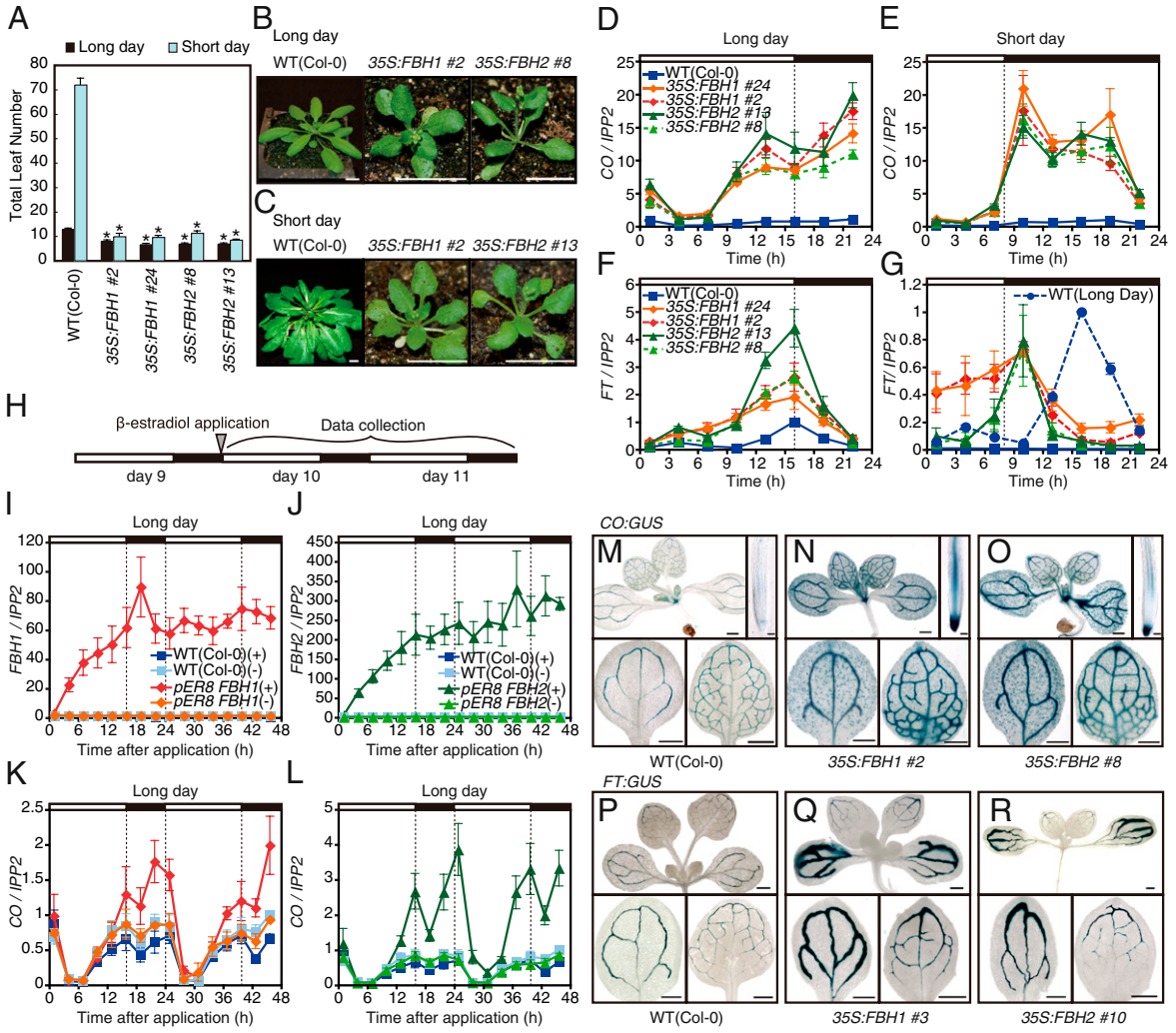

Fig. 2. FBH1 and FBH2 control *CO* expression levels. (*A*) Flowering phenotypes of plants overexpressing *FBH1* (*35S:FBH1*) and *FBH2* (*35S:FBH2*) under different photoperiods. Error bars depict SEM ($n = 6$). Asterisks (*) denote significant difference ($P < 0.001$) between each overexpressor and wild-type plants. The experiment was repeated at least twice, and similar results were obtained. (*B* and *C*) Representative pictures of *35S:FBH* plants in LD (*B*) and SD (*C*). The pictures were taken just after the plants bolted. (*B*) Wild type, 27 d old; *35S:FBH1*, 18 d old; and *35S:FBH2*, 18 d old in LD. (*C*) Wild type, 70 d old; *35S:FBH1*, 28 d old; and *35S:FBH2*, 28 d old in SD. (Scale bars,10 mm.) (*D*–*G*) Daily expression patterns of *CO* (*D* and *E*) and *FT* (*F* and *G*) in *35S:FBH1*, *35S:FBH2*, and wild-type plants in LD and SD. The *FT* expression pattern of wild type in LD (blue dashed line) was superimposed on SD data (*G*). All of the results (*D*–*F*), except *G*, were normalized to the highest values in the wild-type sample (the maximum value of wild type was set to 1). *FT* levels in SD (*G*) were normalized to the peak *FT* expression value in the wild type in LD. (*H*) Seedlings that possess *pER8-FBH1* or *pER8-FBH2* constructs were treated with β-estradiol at day 10 at the onset of light (ZT 0). The arrowhead indicates the start time point of β-estradiol application. Seedlings were harvested starting at 1 h after the onset of light (ZT 1) and then at 3-h intervals for 2 d. (*I*–*L*) *FBH1*, *FBH2*, and *CO* mRNA expression in wild-type plants and *pER8-FBH1* and *pER8-FBH2* transgenic plants after β-estradiol application. The samples treated with and without β-estradiol are indicated by (+) and (–) symbols, respectively. *FBH1* and *FBH2* levels were normalized to the average value in the wild-type (–) sample [the average value from all of the wild-type (–) time points was set to 1]. The *CO* level was normalized to the maximum value of the wild-type (–) sample [the maximum value of wild type (–) was set to 1]. Values represent means ± SEM from three biological replicates in *D*–*G* and in *I*–*L*. The bars above the graphs represent light conditions: white bars, light periods; black bars, dark periods. (*M*–*R*) Spatial expression patterns of *CO* and *FT* gene in *35S:FBH* plants. Twelve-day-old wild-type (*M*), *35S:FBH1* (*N*), and *35S:FBH2* (*O*) plants carrying the *CO:GUS* reporter gene and wild-type (*P*), *35S:FBH1* (*Q*), and *35S:FBH2* (*R*) plants carrying the *FT:GUS* reporter gene were analyzed. Whole-mount staining of seedlings, cotyledons, and the first set of leaves are shown with scale bars (0.5 mm). Staining of root tips is shown with scale bars (0.1 mm).

results indicate that FBH1 and FBH2 activity is somehow restricted to the vascular tissue. We also analyzed the effects of *FBH* overexpression on the spatial pattern of *FT* (Fig. S2 *F* and *G*) and found that GUS activity was strongly enhanced in the *35S:FBH* lines, but the tissue-specific expression pattern of *FT* was not altered (Fig. 2 *P*–*R*). This could be due to the increased levels of *CO* without a large alteration of its spatiotemporal expression pattern in these lines.

FBH1 Binds Near the Transcription Start Site of the *CO* Promoter in Vivo. To understand the mechanism of FBH-dependent *CO* regulation, we examined the spatial expression pattern of *FBH1* by analyzing the *FBH1*-promoter–controlled *GUS* expression pattern (*FBH1:GUS*). We presumed that if FBH1 is a *CO* regulator, its spatial expression pattern should overlap with the *CO* pattern. FBH1:GUS activity was predominantly detected in the vascular tissues (Fig. 3 *A*–*C*), validating our prediction.

Next, we investigated whether FBH1 directly associates with the *CO* promoter in vivo using a chromatin immunoprecipitation (ChIP) assay. For the ChIP assay, we used transgenic plants expressing a FLAG-tagged FBH1 regulated by the *FBH1* promoter (*FBH1:FLAG-FBH1*) and *35S:FLAG-FBH1* plants. First, we confirmed that *CO* levels were elevated in the *FBH1:FLAG-FBH1* and *35S:FLAG-FBH1* lines in a dosage-dependent manner, indicating that the FLAG-FBH1 protein is functional (Fig. S3 *A*–*F*). To investigate FBH1 binding to the *CO* promoter, we harvested LD-grown plants at Zeitgeber time 4 (ZT4) when *CO* expression is at the trough level

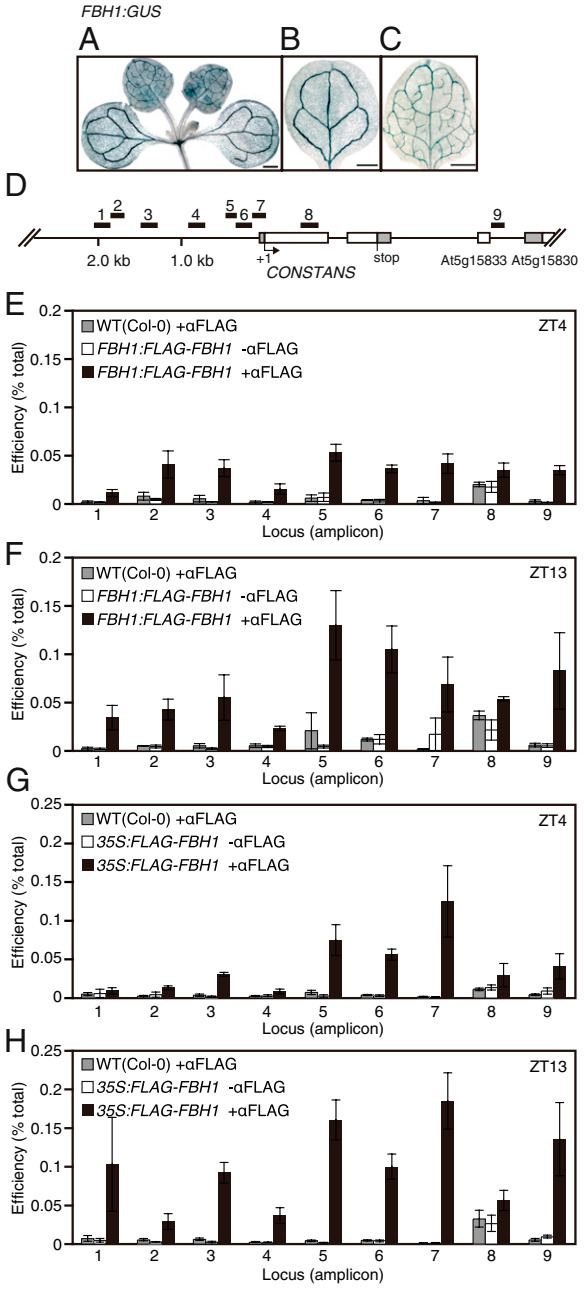

Fig. 3. FBH1 associates with the *CO* promoter. The spatial expression pattern of *FBH1* was determined by histochemical staining of GUS activity in *FBH1:GUS* plants. Whole-mount staining of a seedling (*A*), a cotyledon (*B*), and a first leaf (*C*) are shown. (Scale bars, 0.5 mm.) (*D*) Schematic representation of the *CO* locus and the locations of nine amplicons for ChIP analysis. White and gray boxes represent exons and either 5′- or 3′-UTR. The At5g15833 gene encodes microRNA. (*E*–*H*) Binding of FLAG-FBH1 to the *CO* promoter in vivo. Two-week-old LD-grown seedlings, which possess either *FBH1:FLAG-FBH1* (*E* and *F*) or *35S:FLAG-FBH1* constructs (*G* and *H*) and the wild-type plants were harvested at 4 and 13 h after the onset of light (ZT 4 and ZT 13). ChIP assays were performed using *FLAG-FBH1* plants with the anti-FLAG antibody, *FLAG-FBH1* plants without the antibody, and wild-type plants with the anti-FLAG antibody. The amount of immunoprecipitated DNA was quantified by qPCR using primers specific to each amplicon. Values represent the average immunoprecipitation efficiencies (%) against the total input DNA ± SEM of at least three biological replicates.

and at ZT 13 when daytime *CO* expression is at its peak. We analyzed the FLAG-FBH1–specific enrichment of DNA fragments on different *CO* locations (amplicons 1–9; see Table S3 for detailed information) using quantitative PCR (qPCR) (Fig. 3*D*). In the *FBH1:FLAG-FBH1* plants, FLAG-FBH1–specific enrichment was detected from all chromatin samples harvested at ZT 4 and ZT 13 (Fig. 3 *E* and *F*) with the highest level in amplicons 5, 6, and 7, which are adjacent to the *CO* transcriptional start site. Amplicon 5 (position: −430 to −273) and amplicon 6 (position: −301 to −89), both of which contain one E-box, largely overlap with the region important for the FBH-dependent transcription in yeast (Fig. 1). Amplicon 7 (−89 to +66) also contains one E-box in the 5′-UTR of *CO*. Comparison of the results derived from both time points revealed a higher enrichment in the sample harvested at ZT 13 (Fig. 3 *E* and *F*), which coincides with up-regulation of the *CO* transcript (Fig. S1*E*). Similar trends were observed when we used the *35S:FLAG-FBH1* plants (Fig. 3 *G* and *H*). Together with our yeast one-hybrid and EMSA results, we propose that FBH1 binds to the *CO* chromatin to regulate *CO* transcription in vivo. Because FBH1 protein similarly accumulated throughout the day in LD and SD (Fig. S3 *G*–*I*), FBH1 may require some posttranslational modification or some other unknown proteins to induce *CO* expression.

FBH1 Homologs Have an Overlapping Function as *CO* Activators. To complement our overexpression analysis, we analyzed the mutant phenotype. Because FBH1 and FBH2 have 74% amino-acid-sequence identity and the overexpressors have similar phenotypes, we aimed to obtain an *fbh1 fbh2* double mutant to analyze the loss-of-function phenotype. As only the *FBH2* T-DNA insertion mutant (*fbh2-1*) was available in public collections (Fig. S3*J*), we generated independent *fbh1 fbh2* double-mutant lines in which *FBH1* mRNA was down-regulated by two different artificial microRNA (amiRNA) constructs (*amiRFBH1-1 fbh2-1* and *amiRFBH1-2 fbh2-1*). When we analyzed *CO* and *FT* expression in the *amiRFBH1 fbh2* lines, we did not detect any differences compared with wild-type plants (Fig. S3 *K*–*R*). This result may indicate either that the 10–30% of remaining *FBH1* mRNA is enough to maintain the normal mechanisms of *CO* regulation or that there are yet other proteins (*i.e.*, other relatively closely related bHLH proteins) that function redundantly with FBH1 and FBH2 to compensate for the loss of both genes.

Therefore, we expanded our search for *FBH1* (or *FBH2*) homologs. On the basis of previous phylogenetic analyses, there are four more bHLH genes in the same clade as *FBH1* and *FBH2* (24, 30). The deduced amino acid sequences of these four genes contain highly conserved bHLH domains; however, they have diverse sequences other than the bHLH domains. We successfully cloned three of these bHLHs (At1g51140, At2g42280, and At1g05805) and tested whether they could also induce early flowering when overexpressed. Overexpression of At1g51140 and At2g42280 (named *FBH3* and *FBH4*) also caused an early flowering phenotype (Fig. S4 *A*–*E*). This is likely due to a high amount of *FT* expression (Fig. S4 *F*–*M*) caused by increased *CO* expression in LD and SD (Fig. 4 *A*–*D*). Similar to the *FBH1* and *FBH2* overexpressor phenotypes, the spatial and temporal expression patterns of *CO* were largely restored in the *35S:FBH3* and *35S:FBH4* lines (Fig. 4 *A*–*D* and Fig. S4 *N*–*P*). In addition, yeast one-hybrid analysis demonstrated that FBH3 and FBH4 bind to the same *CO* promoter regions through the E-box elements (Fig. S4 *Q* and *R*).

Temporal expression pattern analysis of all four *FBH* genes revealed that they are expressed throughout the day in LD and SD (Fig. S5 *A*–*H*). *FBH4* (and possibly *FBH1*) transcription showed a diurnal oscillation pattern under constant light conditions (Fig. S5 *B* and *H*), indicating the involvement of circadian-clock regulation. Promoter:*GUS* analysis revealed that the *FBH3* promoter is active mainly in the vascular tissues and that *FBH4* is expressed in the stomata as well as in leaf vascular tissues (Fig. S5 *I*–*K*). Together with the expression pattern analyses, our results indicate that FBH3 and FBH4 have similar functions to FBH1 and FBH2 with regard to *CO* transcriptional regulation.

Because our results indicated that the four FBH proteins might have redundant functions, we analyzed the phenotype of *fbh1 fbh2 fbh3 fbh4* quadruple mutants. To generate the *fbh* quadruple mutants, we used the *FBH1* amiRNA construct, *fbh2-1* (Fig. S3*J*), the *FBH3* T-DNA insertion line (Fig. S6 *A* and *B*), and two *FBH4* amiRNA constructs (*35S:amiRFBH4-1* and *35S:amiRFBH4-3*) (Fig. S6 *C*–*F*). Two independently established quadruple mutant lines [*35S:amiRFBH1-2, fbh2-1, fbh3-1* and

PLANT BIOLOGY

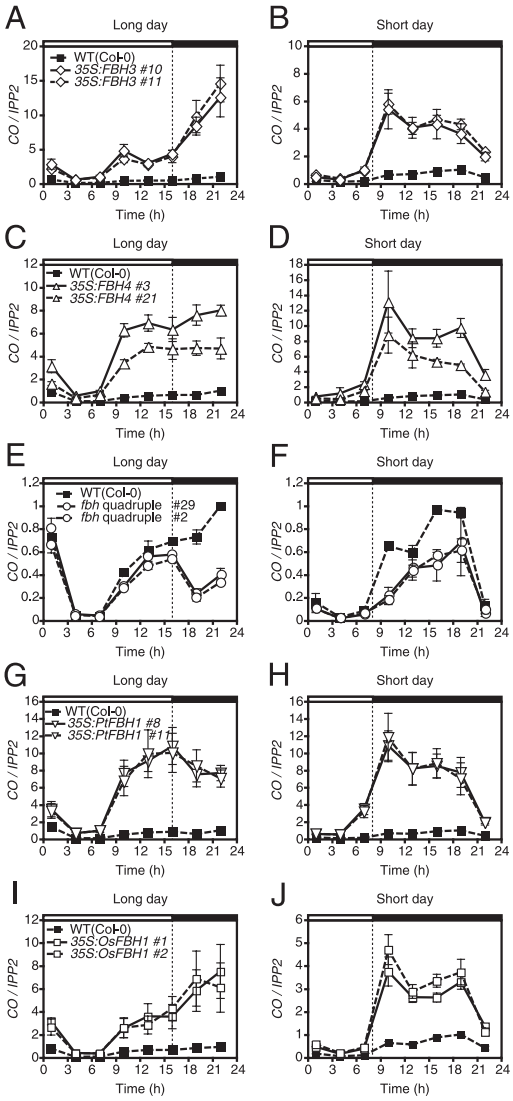

Fig. 4. FBH1 homologs regulate *CO* transcription. (*A–D*) *CO* mRNA expression in *35S:FBH3*, *35S:FBH4*, and wild-type plants in LD and SD. (*E* and *F*) *CO* mRNA expression in two independent *fbh* quadruple mutants and wild-type plants in LD and SD. (*G–J*) *CO* mRNA expression in *Arabidopsis* plants constitutively expressing poplar *FBH* (*35S:PtFBH1*), rice *FBH* (*35S:OsFBH1*), and wild-type plants in LD and SD. All of the results were normalized to the highest value in the wild-type sample. Values represent mean ± SEM from three biological replicates for all experiments.

35S:amiRFBH4-1 (#29) and *35S:amiRFBH1-2, fbh2-1, fbh3-1* and *35S:amiRFBH4-3* (#2)] were chosen for detailed analysis. *CO* expression analysis revealed a larger than 50% reduction of *CO* expression in the first 6 h of the dark periods in LD and SD in the quadruple mutants (Fig. 4 *E* and *F*), suggesting that the FBH proteins are major activators of *CO* especially in the beginning of the night. In LD, there is a slight reduction in afternoon *CO* expression (Fig. 4*E*). This could cause lower expression of *FT* and subsequently later flowering of the quadruple mutants in LD (Fig. S6 *G–J*). These results imply that the four FBH proteins are activators of *CO* transcription in *Arabidopsis*.

***FBH* Genes Are Widely Conserved Activator Genes in the *CO/FT* Flowering Pathway in Plants.** The *CO*/*FT* modules as well as the daily expression patterns of *CO* homologs are widely conserved in many plant species (11). Therefore, we hypothesized that *CO* transcriptional mechanisms including the FBH function might be conserved in other plants. As a primary attempt to examine this hypothesis, we analyzed the function of FBH homologs from poplar (a LD tree) and rice (a SD plant) in *Arabidopsis*. Two representative *FBH* homologs from poplar and rice (named *PtFBH1* and *OsFBH1*, respectively) were chosen on the basis of a homology search and phylogenetic analysis (31) (see the amino acid sequence alignment of FBH1 homologs in Fig. S7 and our phylogenetic analysis in Fig. S8). Overexpression of both *PtFBH1* and *OsFBH1* drastically increased *CO* expression levels in *Arabidopsis* in LD and SD (Fig. 4 *G–J* and Fig. S9 *A–F*). The *35S:PtFBH1* plants showed early flowering in both LD and SD (Fig. S9*G*), and the *35S:OsFBH1* plants showed early flowering in LD (Fig. S9*H*). Because CO protein is constantly degraded in SD (32), the elevated *CO* levels in *35S:OsFBH1* plants may not be sufficiently high to overcome the posttranscriptional regulation of CO in SD. Nevertheless, these results imply that *Pt*FBH1 and *Os*FBH1 have a similar function to *Arabidopsis* FBHs. In addition, there are several E-box elements in 1 kb of the promoter regions of both the poplar and rice *CO* ortholog genes (Fig. S9*I*). This evidence further indicates that *Pt*FBH1 and *Os*FBH1 presumably regulate their own *CO* ortholog expression in poplar and rice, respectively.

Discussion

FBH Proteins Are Transcriptional Activators of *CO*. It is not surprising that multiple redundant factors are involved in *CO* transcriptional regulation because it is the crucial mechanism in the photoperiodic flowering pathway. Interestingly, except for FKF1 and GI, all of the factors currently identified before this work are repressors of *CO* expression (12–21). That may indicate that *CO* activators are highly redundant or also involved in the processes necessary for plant survival. To overcome a potential genetic redundancy, we applied a reverse genetics approach to find additional *CO* regulators (23). We identified that FBH1 directly binds to the *CO* promoter (Figs. 1 and 3); on the basis of homology, we also identified three more bHLH proteins, FBH2, FBH3, and FBH4, which have a similar function to FBH1 (Figs. 2 and 4; and Fig. S4). Our genetic analysis revealed that all of the FBHs are transcriptional activators of *CO*. Ectopic overexpression of *FBH* drastically increased *CO* expression levels but did not alter the spatiotemporal expression patterns of *CO* (Figs. 2 and 4; Fig. S4). These results also let us infer that all of the FBHs may be posttranslationally activated at a specific time of the day mainly in the leaf vasculature and/or may work together with unidentified vascular-specific factors to regulate *CO* transcription.

Circadian-time–dependent activation of transcriptional activators is a conserved mechanism in mammalian, insect, and fungal clock circuits. The mammalian positive circadian regulators, CLOCK and BMAL1, and their insect counterparts, *Drosophila* CLOCK and CYCLE, are bHLH-domain–containing transcriptional activators that induce gene expression of negative regulators (33, 34). Their daily protein expression profiles do not show robust oscillation as negative regulators do; however, the phosphorylation states of these proteins change throughout the day and alter their binding abilities to the *cis*-elements (35, 36). A similar circadian change in the DNA-binding ability of the fungal clock activator WHITE COLLAR complex is also regulated by time-dependent phosphorylation (37). Therefore, one possible posttranslational mechanism that controls FBH function could be phosphorylation-dependent changes in DNA-binding abilities.

The latter possibility is also supported by our data. In the quadruple mutants in LD, two distinct peaks of *CO* (at around ZT 13 and at dawn) were observed (Fig. 4*E*). Because *FBH* overexpression drastically elevated *CO* levels from afternoon to night in LD (Fig. 2 *D* and *E* and Fig. 4 *A–D*), this result implies that other functionally redundant transcriptional activators contribute to the regulation of LD-specific daytime *CO* expression (as well as the end-of-night *CO* expression). Because the expression of *FBH* mRNAs and FBH1 protein do not show robust daily oscillation (Figs. S3 and S5), time-dependent changes in FBH activity could also be regulated by the potential spatiotemporal expression of the coactivators. Our next challenges will be to identify other

coactivators of *CO* and also to decipher the molecular relationship between multiple *CO* regulators and FBH function in terms of controlling the precise timing of daily *CO* expression.

Our results indicate that *FBH* levels regulate the amplitude of daily *CO* oscillation. Even changing the amplitude of *CO* expression altered overall *FT* levels (Fig. 2). This implies that plants can regulate not only the timing of *CO* expression but also the amount of *CO* levels to control the overall amount of *FT*. Having redundant FBH proteins may enable *Arabidopsis* plants to accurately tune the expression level of *CO* as well as to increase a dynamic range of *CO* expression levels by regulating four different *FBH* expressions, so that plants can respond to various internal and external conditions more precisely and robustly for flowering.

***FBH* Homologs May Regulate *CO* Orthologs in Other Plant Species.** Our study also suggests that FBH homologs may function as transcriptional activators of *CO* homologs in other plants. The daily expression patterns of *CO* orthologs are very similar (11), indicating that transcriptional regulatory mechanisms may be also conserved. We demonstrated that *Pt*FBH1 (poplar FBH) and *Os*FBH1 (rice FBH) have a similar function to FBHs in *Arabidopsis* (Fig. 4). Our phylogenetic analysis indicated that there is at least one (usually more) bHLH that belongs to the same clade of FBH (designated as IX, Fig. S8) in all angiosperms (*Arabidopsis*, poplar, rice, tomato, maize, and grape) examined. In addition, we found that the multiple E-box elements (but not G-boxes) exist on 1-kb upstream regions of the *PtCO2* and *Hd1* promoters (Fig. S9*I*). These results also indicate that E-box–binding factors (possibly bHLHs in the FBH clade) may participate in the *CO* transcriptional regulation. Although it is beyond the scope of this current analysis, it would be intriguing to test the function of *Pt*FBH1 and *Os*FBH1 in poplar and rice, respectively.

In summary, our data indicate that, together with circadian-clock–regulated repressors, plants may possess overlapping mechanisms to regulate the expression levels of *CO* (and *CO* orthologs) by a group of related transcriptional activators to precisely regulate the timing of expression for successful reproduction.

Materials and Methods

The Colombia-0 accession was used as wild type for all experiments. The *ft-101* mutant was described previously (28). Procedures for *A. thaliana* husbandry; yeast one-hybrid, EMSA, and ChIP assays; and the GUS-staining experiment were described previously (38–41) and were carried out with modifications detailed in the *SI Materials and Methods*. *FBH1*, *FBH2*, *FBH3*, *FBH4*, *PtFBH1*, and *OsFBH1* coding regions were cloned into the pB7WG2 binary vector to generate each overexpressor line. For making the amiRNA constructs that specifically reduce the amount of *FBH1* and *FBH4* mRNA, specific *FBH1*- and *FBH4*-targeted amiRNA sequences were introduced into the miR319 backbone plasmid (pRS300). The resulting 35S-promoter–driven *FBH1* and *FBH4* amiRNA expression cassettes were cloned into pPZP221 or pH7WG2 binary vectors, respectively. *FBH1* and *FBH2* β-estradiol–inducible lines were generated by transformation with the pER8 plasmid containing the *FBH1* and *FBH2* coding regions. For expression analysis, seedlings were grown on plates containing 1× Linsmaier and Skoog media (Caisson) containing 3% sucrose under LD, SD, or 12 h light/12 h dark conditions for 10 d and harvested. The gene expression levels were measured by qPCR analyses. Detailed information is provided in *SI Materials and Methods*. All primer sequences used in this project are listed in Tables S1–S3.

ACKNOWLEDGMENTS. We thank S. Kay for constant encouragement, initial support, and the transcription factor library; E. Farré and J. Pruneda-Paz for critical reading of the manuscript; J. Pruneda-Paz and S. Kay for sharing unpublished results; K. Goto for Arabidopsis lines; and N.-H. Chua and K. Torii for plasmids. S.I. was supported by a Japan Society for the Promotion of Science Postdoctoral Fellowship. Y.H.S. is partly supported by the Next Generation Biogreen 21 Program (PJ008109). This work was supported by National Institutes of Health Grant GM079712 (to T.I.).

1. Thomas B, Vince-Prue D (1996) *Photoperiodism in Plants* (Academic Press, New York).
2. Yanovsky MJ, Kay SA (2003) Living by the calendar: How plants know when to flower. *Nat Rev Mol Cell Biol* 4:265–275.
3. Kobayashi Y, Weigel D (2007) Move on up, it's time for change—Mobile signals controlling photoperiod-dependent flowering. *Genes Dev* 21:2371–2384.
4. Amasino R (2010) Seasonal and developmental timing of flowering. *Plant J* 61:1001–1013.
5. de Montaigu A, Tóth R, Coupland G (2010) Plant development goes like clockwork. *Trends Genet* 26:296–306.
6. Imaizumi T (2010) Arabidopsis circadian clock and photoperiodism: Time to think about location. *Curr Opin Plant Biol* 13:83–89.
7. Corbesier L, et al. (2007) FT protein movement contributes to long-distance signaling in floral induction of *Arabidopsis*. *Science* 316:1030–1033.
8. Abe M, et al. (2005) FD, a bZIP protein mediating signals from the floral pathway integrator FT at the shoot apex. *Science* 309:1052–1056.
9. Wigge PA, et al. (2005) Integration of spatial and temporal information during floral induction in *Arabidopsis*. *Science* 309:1056–1059.
10. Böhlenius H, et al. (2006) *CO/FT* regulatory module controls timing of flowering and seasonal growth cessation in trees. *Science* 312:1040–1043.
11. Song YH, Ito S, Imaizumi T (2010) Similarities in the circadian clock and photoperiodism in plants. *Curr Opin Plant Biol* 13:594–603.
12. Fowler S, et al. (1999) *GIGANTEA*: A circadian clock-controlled gene that regulates photoperiodic flowering in *Arabidopsis* and encodes a protein with several possible membrane-spanning domains. *EMBO J* 18:4679–4688.
13. Suárez-López P, et al. (2001) *CONSTANS* mediates between the circadian clock and the control of flowering in *Arabidopsis*. *Nature* 410:1116–1120.
14. Imaizumi T, Tran HG, Swartz TE, Briggs WR, Kay SA (2003) FKF1 is essential for photoperiodic-specific light signalling in *Arabidopsis*. *Nature* 426:302–306.
15. Imaizumi T, Schultz TF, Harmon FG, Ho LA, Kay SA (2005) FKF1 F-box protein mediates cyclic degradation of a repressor of *CONSTANS* in *Arabidopsis*. *Science* 309:293–297.
16. Mizoguchi T, et al. (2005) Distinct roles of *GIGANTEA* in promoting flowering and regulating circadian rhythms in Arabidopsis. *Plant Cell* 17:2255–2270.
17. Chen M, Ni M (2006) RFI2, a RING-domain zinc finger protein, negatively regulates *CONSTANS* expression and photoperiodic flowering. *Plant J* 46:823–833.
18. Yoo SY, Kim Y, Kim SY, Lee JS, Ahn JH (2007) Control of flowering time and cold response by a NAC-domain protein in *Arabidopsis*. *PLoS ONE* 2:e642.
19. Kim J, Kim Y, Yeom M, Kim JH, Nam HG (2008) FIONA1 is essential for regulating period length in the *Arabidopsis* circadian clock. *Plant Cell* 20:307–319.
20. Wu JF, Wang Y, Wu SH (2008) Two new clock proteins, LWD1 and LWD2, regulate Arabidopsis photoperiodic flowering. *Plant Physiol* 148:948–959.
21. Fornara F, et al. (2009) *Arabidopsis* DOF transcription factors act redundantly to reduce *CONSTANS* expression and are essential for a photoperiodic flowering response. *Dev Cell* 17:75–86.
22. Sawa M, Nusinow DA, Kay SA, Imaizumi T (2007) FKF1 and GIGANTEA complex formation is required for day-length measurement in *Arabidopsis*. *Science* 318:261–265.
23. Pruneda-Paz JL, Breton G, Para A, Kay SA (2009) A functional genomics approach reveals CHE as a component of the *Arabidopsis* circadian clock. *Science* 323:1481–1485.
24. Toledo-Ortiz G, Huq E, Quail PH (2003) The Arabidopsis basic/helix-loop-helix transcription factor family. *Plant Cell* 15:1749–1770.
25. Onouchi H, Igeño MI, Périlleux C, Graves K, Coupland G (2000) Mutagenesis of plants overexpressing CONSTANS demonstrates novel interactions among Arabidopsis flowering-time genes. *Plant Cell* 12:885–900.
26. Michaels SD, Amasino RM (1999) *FLOWERING LOCUS C* encodes a novel MADS domain protein that acts as a repressor of flowering. *Plant Cell* 11:949–956.
27. Zuo J, Niu QW, Chua NH (2000) Technical advance: An estrogen receptor-based transactivator XVE mediates highly inducible gene expression in transgenic plants. *Plant J* 24:265–273.
28. Takada S, Goto K (2003) Terminal flower2, an Arabidopsis homolog of heterochromatin protein1, counteracts the activation of *flowering locus T* by constans in the vascular tissues of leaves to regulate flowering time. *Plant Cell* 15:2856–2865.
29. An H, et al. (2004) CONSTANS acts in the phloem to regulate a systemic signal that induces photoperiodic flowering of Arabidopsis. *Development* 131:3615–3626.
30. Pires N, Dolan L (2010) Origin and diversification of basic-helix-loop-helix proteins in plants. *Mol Biol Evol* 27:862–874.
31. Carretero-Paulet L, et al. (2010) Genome-wide classification and evolutionary analysis of the bHLH family of transcription factors in Arabidopsis, poplar, rice, moss, and algae. *Plant Physiol* 153:1398–1412.
32. Valverde F, et al. (2004) Photoreceptor regulation of CONSTANS protein in photoperiodic flowering. *Science* 303:1003–1006.
33. Glossop NR, Lyons LC, Hardin PE (1999) Interlocked feedback loops within the Drosophila circadian oscillator. *Science* 286:766–768.
34. Gekakis N, et al. (1998) Role of the CLOCK protein in the mammalian circadian mechanism. *Science* 280:1564–1569.
35. Yoshitane H, et al. (2009) Roles of CLOCK phosphorylation in suppression of E-box-dependent transcription. *Mol Cell Biol* 29:3675–3686.
36. Yu W, Zheng H, Houl JH, Dauwalder B, Hardin PE (2006) PER-dependent rhythms in CLK phosphorylation and E-box binding regulate circadian transcription. *Genes Dev* 20:723–733.
37. He Q, et al. (2006) CKI and CKII mediate the FREQUENCY-dependent phosphorylation of the WHITE COLLAR complex to close the Neurospora circadian negative feedback loop. *Genes Dev* 20:2552–2565.
38. Sieburth LE, Meyerowitz EM (1997) Molecular dissection of the AGAMOUS control region shows that cis elements for spatial regulation are located intragenically. *Plant Cell* 9:355–365.
39. Deplancke B, et al. (2006) A gene-centered C. elegans protein-DNA interaction network. *Cell* 125:1193–1205.
40. Song YH, et al. (2008) Isolation of CONSTANS as a TGA4/OBF4 interacting protein. *Mol Cells* 25:559–565.
41. Almada R, Cabrera N, Casaretto JA, Ruiz-Lara S, González Villanueva E (2009) VvCO and VvCOL1, two CONSTANS homologous genes, are regulated during flower induction and dormancy in grapevine buds. *Plant Cell Rep* 28:1193–1203.